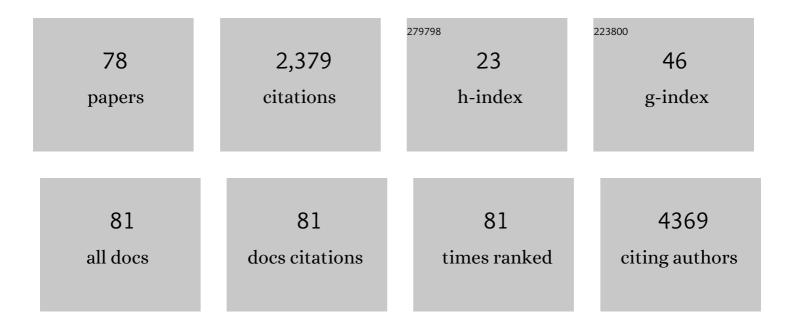


List of Publications by Year in descending order

Source: https://exaly.com/author-pdf/7727680/publications.pdf Version: 2024-02-01



#	Article	IF	CITATIONS
1	Posterior corneal elevation changes and characteristic analysis 1Âyear after corneal collagen cross-linking for keratoconus. International Ophthalmology, 2022, 42, 1457-1468.	1.4	1
2	Selfâ€Organization of Tissue Growth by Interfacial Mechanical Interactions in Multilayered Systems. Advanced Science, 2022, 9, e2104301.	11.2	3
3	Bagâ€1 mediates glucocorticoid receptor trafficking to mitochondria after corticosterone stimulation: Potential role in regulating affective resilience. Journal of Neurochemistry, 2021, 158, 358-372.	3.9	9
4	Ganoderic Acid A Attenuates LPS-Induced Neuroinflammation in BV2 Microglia by Activating Farnesoid X Receptor. Neurochemical Research, 2021, 46, 1725-1736.	3.3	19
5	Ganoderic acid A exerted antidepressant-like action through FXR modulated NLRP3 inflammasome and synaptic activity. Biochemical Pharmacology, 2021, 188, 114561.	4.4	22
6	Extracellular Matrix Stiffness Regulates DNA Methylation by PKC α â€Dependent Nuclear Transport of DNMT3L. Advanced Healthcare Materials, 2021, 10, 2100821.	7.6	11
7	Ganoderma lucidum polysaccharides ameliorated depression-like behaviors in the chronic social defeat stress depression model via modulation of Dectin-1 and the innate immune system. Brain Research Bulletin, 2021, 171, 16-24.	3.0	26
8	Magical oxygen: Tuning Cu&Ag nanoporous membrane into nanoporous (Cu&Ag)@Ag core-shell alloy. Physica B: Condensed Matter, 2021, 614, 413011.	2.7	4
9	Soft substrate and decreased cytoskeleton contractility promote coupling and morphology maintenance of pluripotent stem cells. Acta Mechanica Sinica/Lixue Xuebao, 2021, 37, 1520-1529.	3.4	1
10	2020 update on human coronaviruses: One health, one world. Medicine in Novel Technology and Devices, 2020, 8, 100043.	1.6	21
11	Hollow Bimetallic Complex Nanoparticles for Trimodality Imaging and Photodynamic Therapy In Vivo. ACS Applied Materials & Interfaces, 2020, 12, 37470-37476.	8.0	14
12	Targeted gold nanoshelled hybrid nanocapsules encapsulating doxorubicin for bimodal imaging and near-infrared triggered synergistic therapy of Her2-positve breast cancer. Journal of Biomaterials Applications, 2020, 35, 430-445.	2.4	11
13	Oridonin is an antidepressant molecule working through the PPAR-γ/AMPA receptor signaling pathway. Biochemical Pharmacology, 2020, 180, 114136.	4.4	12
14	The Authors' Reply: Comment on: BRAF mutation analysis by ARMSâ€PCR refines thyroid nodule management. Clinical Endocrinology, 2020, 92, 483-485.	2.4	0
15	<p>Her2-Targeted Multifunctional Nano-Theranostic Platform Mediates Tumor Microenvironment Remodeling and Immune Activation for Breast Cancer Treatment</p> . International Journal of Nanomedicine, 2020, Volume 15, 10007-10028.	6.7	28
16	Classification of Subcortical Vascular Cognitive Impairment Using Single MRI Sequence and Deep Learning Convolutional Neural Networks. Frontiers in Neuroscience, 2019, 13, 627.	2.8	12
17	Cordycepin (3′-deoxyadenosine) promotes remyelination via suppression of neuroinflammation in a cuprizone-induced mouse model of demyelination. International Immunopharmacology, 2019, 75, 105777.	3.8	17
18	Compression Generated by a 3D Supracellular Actomyosin Cortex Promotes Embryonic Stem Cell Colony Growth and Expression of Nanog and Oct4. Cell Systems, 2019, 9, 214-220.e5.	6.2	20

#	Article	IF	CITATIONS
19	Activation of AMPK promotes thyroid cancer cell migration through its interaction with PKM2 and β-catenin. Life Sciences, 2019, 239, 116877.	4.3	9
20	<i>BRAF</i> mutation analysis by ARMSâ€₽CR refines thyroid nodule management. Clinical Endocrinology, 2019, 91, 834-841.	2.4	20
21	Comparisons and Combined Application of Two-Dimensional and Three-Dimensional Real-time Shear Wave Elastography in Diagnosis of Thyroid Nodules. Journal of Cancer, 2019, 10, 1975-1984.	2.5	14
22	Characterizing the Penumbras of White Matter Hyperintensities and Their Associations With Cognitive Function in Patients With Subcortical Vascular Mild Cognitive Impairment. Frontiers in Neurology, 2019, 10, 348.	2.4	26
23	Structural brain network measures are superior to vascular burden scores in predicting early cognitive impairment in post stroke patients with small vessel disease. NeuroImage: Clinical, 2019, 22, 101712.	2.7	39
24	Her2-Functionalized Gold-Nanoshelled Magnetic Hybrid Nanoparticles: a Theranostic Agent for Dual-Modal Imaging and Photothermal Therapy of Breast Cancer. Nanoscale Research Letters, 2019, 14, 235.	5.7	45
25	A Maitake (<i>Grifola frondosa</i>) polysaccharide ameliorates Alzheimer's disease-like pathology and cognitive impairments by enhancing microglial amyloid-l² clearance. RSC Advances, 2019, 9, 37127-37135.	3.6	25
26	A Polysaccharide Extract from Maitake Culinary-Medicinal Mushroom, Grifola frondosa (Agaricomycetes) Ameliorates Learning and Memory Function in Aluminum Chloride-Induced Amnesia in Mice. International Journal of Medicinal Mushrooms, 2019, 21, 1065-1074.	1.5	7
27	Contrasting effects of acute and long-term corticosterone treatment on amyloid-Î ² , beta-secretase 1 expression, and nuclear factor kappa B nuclear translocation. Journal of Integrative Neuroscience, 2019, 18, 393.	1.7	2
28	Au-poly(lactic-co-glycolic) acid complex nanoparticles as ultrasound contrast agents: Preparation, characterization and inÃ-Â;½vitro study. Molecular Medicine Reports, 2018, 17, 3763-3768.	2.4	6
29	Preparation and Imaging Investigation of Dual-targeted C3F8-filled PLGA Nanobubbles as a Novel Ultrasound Contrast Agent for Breast Cancer. Scientific Reports, 2018, 8, 3887.	3.3	35
30	Preliminary Results of Acoustic Radiation Force Impulse Imaging by Combined Qualitative and Quantitative Analyses for Evaluation of Breast Lesions. Journal of Ultrasound in Medicine, 2018, 37, 2405-2412.	1.7	7
31	Salmonella osteomyelitis in a previously healthy neonate: a case report and review of the literature. Italian Journal of Pediatrics, 2018, 44, 28.	2.6	7
32	Effects of mechanical stretch on the functions of BK and L-type Ca2+ channels in vascular smooth muscle cells. Journal of Biomechanics, 2018, 67, 18-23.	2.1	11
33	Contrast-enhanced ultrasonography for assessment of tubular atrophy/interstitial fibrosis in immunoglobulin A nephropathy: a preliminary clinical study. Abdominal Radiology, 2018, 43, 1423-1431.	2.1	4
34	Ultrasound molecular imaging of breast cancer in MCF-7 orthotopic mice using gold nanoshelled poly(lactic-co-glycolic acid) nanocapsules: a novel dual-targeted ultrasound contrast agent. International Journal of Nanomedicine, 2018, Volume 13, 1791-1807.	6.7	17
35	Assessment of the use of contrast enhanced ultrasound in guiding microdissection testicular sperm extraction in nonobstructive azoospermia. BMC Urology, 2018, 18, 48.	1.4	9
36	The utility and limitations of contrast-enhanced transrectal ultrasound scanning for the detection of prostate cancer in different area of prostate. Clinical Hemorheology and Microcirculation, 2018, 70, 281-290.	1.7	2

#	Article	IF	CITATIONS
37	Synthesis, characterization, and <i>in vitro</i> evaluation of targeted gold nanoshelled poly(<scp>d</scp> , <scp>l</scp> -lactide-co-glycolide) nanoparticles carrying anti p53 antibody as a theranostic agent for ultrasound contrast imaging and photothermal therapy. Journal of Biomaterials Science, Polymer Edition, 2017, 28, 415-430.	3.5	23
38	PEGylated graphene oxide elicits strong immunological responses despite surface passivation. Nature Communications, 2017, 8, 14537.	12.8	157
39	A Role of BK Channel in Regulation of Ca 2+ Channel in Ventricular Myocytes by Substrate Stiffness. Biophysical Journal, 2017, 112, 1406-1416.	0.5	12
40	A Dynamic Biochemomechanical Model of Geometry-Confined Cell Spreading. Biophysical Journal, 2017, 112, 2377-2386.	0.5	14
41	<i>Griflola frondosa</i> (GF) produces significant antidepressant effects involving AMPA receptor activation in mice. Pharmaceutical Biology, 2017, 55, 299-305.	2.9	2
42	One-pot preparation of nanoporous Ag-Cu@Ag core-shell alloy with enhanced oxidative stability and robust antibacterial activity. Scientific Reports, 2017, 7, 10249.	3.3	29
43	Enhanced delivery of biodegradable mPEG-PLGA-PLL nanoparticles loading Cy3-labelled PDGF-BB siRNA by UTMD to rat retina. Journal of Biosciences, 2017, 42, 299-309.	1.1	14
44	Lentinan produces a robust antidepressant-like effect via enhancing the prefrontal Dectin-1/AMPA receptor signaling pathway. Behavioural Brain Research, 2017, 317, 263-271.	2.2	24
45	The Role of Nutrients in Protecting Mitochondrial Function and Neurotransmitter Signaling: Implications for the Treatment of Depression, PTSD, and Suicidal Behaviors. Critical Reviews in Food Science and Nutrition, 2016, 56, 2560-2578.	10.3	78
46	AÎ ² Metabolism and the Role of APOE in Alzheimer's Disease. , 2016, 06, .		1
47	Classification of Benign and Malignant Thyroid Nodules Using a Combined Clinical Information and Gene Expression Signatures. PLoS ONE, 2016, 11, e0164570.	2.5	11
48	Extracellular matrix stiffness dictates Wnt expression through integrin pathway. Scientific Reports, 2016, 6, 20395.	3.3	155
49	Preparation of pH-responsive hollow poly(MAA-co-EGDMA) nanocapsules for drug delivery and ultrasound imaging. RSC Advances, 2016, 6, 103754-103762.	3.6	9
50	Overexpression of miR-30a in lung adenocarcinoma A549 cell line inhibits migration and invasion via targeting <italic>EYA2</italic> . Acta Biochimica Et Biophysica Sinica, 2016, 48, 220-228.	2.0	30
51	3'-Deoxyadenosine (Cordycepin) Produces a Rapid and Robust Antidepressant Effect via Enhancing Prefrontal AMPA Receptor Signaling Pathway. International Journal of Neuropsychopharmacology, 2016, 19, pyv112.	2.1	22
52	Preoperative Diagnosis of Papillary Thyroid Cancer and Lymph Node Metastasis Risk Evaluation Using Clinical Information-Based Bioinformatics Models. Journal of Computational and Theoretical Nanoscience, 2016, 13, 8383-8391.	0.4	0
53	Synthesis, characterization and in vitro and in vivo investigation of C3F8-filled poly(lactic-co-glycolic) Tj ETQq1 1	0.784314 2.4	rgBT /Overic
54	Risk given by <i>AGT</i> polymorphisms in inducing susceptibility to essential hypertension among isolated populations from a remote region of China: A case-control study among the isolated populations. JRAAS - Journal of the Renin-Angiotensin-Aldosterone System, 2015, 16, 1202-1217.	1.7	4

nonulations IDAAS Journa	of the Penin-Angiotensin-Alde	osterone System, 2015, 16, 1202-12
populacions, jichts - journa	of the Kenni-Anglotensin-Alu	osterone System, 2015, 10, 1202-17

#	Article	IF	CITATIONS
55	Lifeact and Utr230 induce distinct actin assemblies in cell nuclei. Cytoskeleton, 2015, 72, 570-575.	2.0	20
56	Novel Cu–Ag bimetallic porous nanomembrane prepared from a multi-component metallic glass. RSC Advances, 2015, 5, 50565-50571.	3.6	12
57	Differential Diagnosis of Polypoid Lesions of the Gallbladder Using Contrastâ€Enhanced Sonography. Journal of Ultrasound in Medicine, 2015, 34, 1061-1069.	1.7	20
58	Radiofrequency Ablation for Hepatocellular Carcinoma: Utility of Conventional Ultrasound and Contrast-Enhanced Ultrasound in Guiding and Assessing Early Therapeutic Response and Short-Term Follow-Up Results. Ultrasound in Medicine and Biology, 2015, 41, 2400-2411.	1.5	32
59	Binding of integrin α1 to bone morphogenetic protein receptor IA suggests a novel role of integrin α1β1 in bone morphogenetic protein 2 signalling. Journal of Biomechanics, 2015, 48, 3950-3954.	2.1	9
60	Integrin activation and internalization mediated by extracellular matrix elasticity: A biomechanical model. Journal of Biomechanics, 2014, 47, 1479-1484.	2.1	31
61	Paramagnetic hollow silica nanospheres for inÂvivo targeted ultrasound and magnetic resonance imaging. Biomaterials, 2014, 35, 5381-5392.	11.4	71
62	Prostate stem cell antigen antibody-conjugated multiwalled carbon nanotubes for targeted ultrasound imaging and drug delivery. Biomaterials, 2014, 35, 5369-5380.	11.4	162
63	A rapid in situ immobilization of d-amino acid oxidase based on immobilized metal affinity chromatography. Bioprocess and Biosystems Engineering, 2014, 37, 857-864.	3.4	6
64	Trehalose rescues Alzheimer's disease phenotypes in APP/PS1 transgenic mice. Journal of Pharmacy and Pharmacology, 2013, 65, 1753-1756.	2.4	112
65	Influence of Serum Prostate-Specific Antigen (PSA) Level, Prostate Volume, and PSA Density on Prostate Cancer Detection With Contrast-Enhanced Sonography Using Contrast-Tuned Imaging Technology. Journal of Ultrasound in Medicine, 2013, 32, 741-748.	1.7	5
66	Differentiating benign from malignant solid breast lesions: Combined utility of conventional ultrasound and contrast-enhanced ultrasound in comparison with magnetic resonance imaging. European Journal of Radiology, 2012, 81, 3890-3899.	2.6	67
67	Biocompatiable hollow silica microspheres as novel ultrasound contrast agents for in vivo imaging. Journal of Materials Chemistry, 2011, 21, 6576.	6.7	76
68	Integrin activation and internalization on soft ECM as a mechanism of induction of stem cell differentiation by ECM elasticity. Proceedings of the National Academy of Sciences of the United States of America, 2011, 108, 9466-9471.	7.1	302
69	Differential Diagnosis of Azoospermia and Etiologic Classification of Obstructive Azoospermia: Role of Scrotal and Transrectal US. Radiology, 2010, 256, 493-503.	7.3	42
70	PPAR ^{ĵ3} transcriptionally regulates the expression of insulin-degrading enzyme in primary neurons. Biochemical and Biophysical Research Communications, 2009, 383, 485-490.	2.1	61
71	Antagonist of peroxisome proliferator-activated receptor Î ³ induces cerebellar amyloid-Î ² levels and motor dysfunction in APP/PS1 transgenic mice. Biochemical and Biophysical Research Communications, 2009, 384, 357-361.	2.1	19
72	Therapeutic potential of lipase inhibitor orlistat in Alzheimer's disease. Medical Hypotheses, 2009, 73, 662-663.	1.5	14

#	Article	IF	CITATIONS
73	ApoE 4 reduces the expression of Aβ degrading enzyme IDE by activating the NMDA receptor in hippocampal neurons. Neuroscience Letters, 2009, 464, 140-145.	2.1	27
74	Expression of TRPM8 in the distal cerebrospinal fluid-contacting neurons in the brain mesencephalon of rats. Cerebrospinal Fluid Research, 2009, 6, 3.	0.5	23
75	Metabolites of Cerebellar Neurons and Hippocampal Neurons Play Opposite Roles in Pathogenesis of Alzheimer's Disease. PLoS ONE, 2009, 4, e5530.	2.5	14
76	Correlation of Real-time Gray Scale Contrast-Enhanced Ultrasonography With Microvessel Density and Vascular Endothelial Growth Factor Expression for Assessment of Angiogenesis in Breast Lesions. Journal of Ultrasound in Medicine, 2008, 27, 821-831.	1.7	54
77	Microvascular Architecture of Breast Lesions. Journal of Ultrasound in Medicine, 2008, 27, 833-842.	1.7	78
78	ls it important to measure the internal spermatic vein diameter after varicocelectomy? A selfâ $\in\!\!\!\varepsilon$ ontrolled trial. Andrologia, 0, , .	2.1	0